Journal Pre-proof

A novel phenylalanine ammonia-lyase from *Pseudozyma antarctica* for stereoselective biotransformations of unnatural amino acids

Andrea Varga (Investigation) (Methodology) (Writing - review and editing) (Writing - original draft), Pál Csuka (Investigation) (Writing - review and editing), Orlavanah Sonesouphap (Investigation), Gergely Bánóczi (Software) (Visualization), Monica Ioana Toşa (Methodology) (Project administration) (Formal analysis), Gabriel Katona (Validation) (Resources), Zsófia Molnár (Investigation), László Csaba Bencze (Writing - review and editing) (Supervision), László Poppe (Conceptualization) (Writing - review and editing) (Supervision) (Project administration) (Funding acquisition), Csaba Paizs (Conceptualization) (Methodology) (Project administration) (Supervision) (Writing - review and editing)

PII: S0920-5861(20)30190-5

DOI: https://doi.org/10.1016/j.cattod.2020.04.002

Reference: CATTOD 12781

To appear in: *Catalysis Today*

Received Date: 2 December 2019

Revised Date: 30 March 2020

Accepted Date: 1 April 2020

Please cite this article as: Varga A, Csuka P, Sonesouphap O, Bánóczi G, Toşa MI, Katona G, Molnár Z, Bencze LC, Poppe L, Paizs C, A novel phenylalanine ammonia-lyase from *Pseudozyma antarctica* for stereoselective biotransformations of unnatural amino acids, *Catalysis Today* (2020), doi: https://doi.org/10.1016/j.cattod.2020.04.002

A novel phenylalanine ammonia-lyase from *Pseudozyma antarctica* for stereoselective biotransformations of unnatural amino acids

Andrea Varga[a], Pál Csuka[b], Orlavanah Sonesouphap[a,c], Gergely Bánóczi[a], Monica Ioana Toșa[a], Gabriel Katona[a], Zsófia Molnár[b], László Csaba Bencze*[a], László Poppe*[a,b,d], Csaba Paizs*[a]

[a]*Biocatalysis and Biotransformation Research Center, Faculty of Chemistry and Chemical Engineering, Babeş-Bolyai University of Cluj-Napoca, Arany János str. 11, 400028, Cluj-Napoca, Romania,*
[b]*Department of Organic Chemistry and Technology, Budapest University of Technology and Economics, Műegyetem rkp. 3, 1111, Budapest, Hungary*
[c]*Department of Chemical Engineering, Faculty of Engineering, National University of Laos, P.O.Box: 7322, Dongdok, Laos*
[d]*SynBiocat Ltd, Szilasliget u. 3, 1172, Budapest, Hungary*

Corresponding authors:

Csaba Paizs
E-mail:paizs@chem.ubbcluj.ro

László Poppe
E-mail:poppe@mail.bme.hu

László Csaba Bencze
E-mail:cslbencze@chem.ubbcluj.ro

Graphical abstract

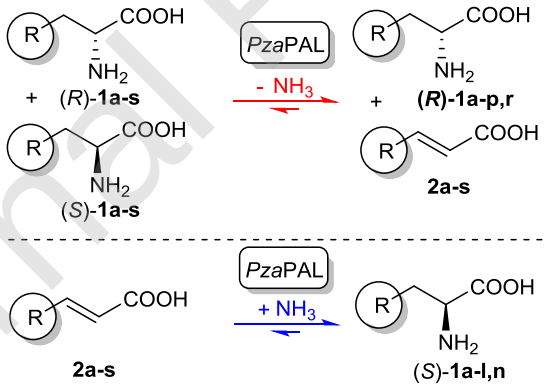

Highlights

- Novel phenylalanine ammonia-lyase for the production of unnatural amino acids;
- Superior turnover numbers compared to known phenylalanine ammonia-lyases;
- Superior enantioselectivity in the synthesis of unnatural phenylalanines bearing electron withdrawing substituents;
- High thermal stability for an enzyme of psychrophilic origin.

Abstract

A novel phenylalanine ammonia-lyase of the psychrophilic yeast *Pseudozyma antarctica* (*Pza*PAL) was identified by screening microbial genomes against known PAL sequences. *Pza*PAL has a significantly different substrate binding pocket with an extended loop (26 aa long) connected to the aromatic ring binding region of the active site as compared to the known PALs from eukaryotes. The general properties of recombinant *Pza*PAL expressed in *E. coli* were characterized including kinetic features of this novel PAL with L-phenylalanine (*S*)-**1a** and further racemic substituted phenylalanines *rac*-**1b-g,k**. In most cases, *Pza*PAL revealed significantly higher turnover numbers than the PAL from *Petroselinum crispum* (*Pc*PAL). Finally, the biocatalytic performance of *Pza*PAL and *Pc*PAL was compared in the kinetic resolutions of racemic phenylalanine derivatives (*rac*-**1a-s**) by enzymatic ammonia elimination and also in the enantiotope selective ammonia addition reactions to cinnamic acid derivatives (**2a-s**). The enantiotope selectivity of *Pza*PAL with *o*-, *m*-, *p*-fluoro-, *o*-, *p*-chloro- and *o*-, *m*-bromo-substituted cinnamic acids proved to be higher than that of *Pc*PAL.

Keywords
biocatalysis; phenylalanine ammonia-lyase; yeast; *Pseudozyma antarctica*; unnatural amino acid

1. Introduction

The pharmaceutical industry is in an ever-growing need for enantiopure compounds and more effective synthetic routes.[1] Biocatalysts being related almost exclusively to enzymes are eco-friendly biomaterials with high application potential in synthetic chemistry.[2] Enzymes can catalyze stereoselective reactions resulting in various building blocks, intermediates or active pharmaceutical ingredients (APIs) of high value.[3] It is an excellent choice to utilize the benefits of biocatalysis in production of enantiopure API molecules.

Enantiopure aromatic α- and β-amino acids are frequently occurring building blocks of natural secondary metabolites such as andrimide,[4] enedyine C-1027,[5] taxol,[6,7] chondramide C, L-DOPA[8] or L-thyroxine. Thus, enantiopure α- and β-amino acids and their unnatural analogues are well-applicable precursors of nuclear hormone inhibitors, hepatitis C antiviral agents or cholecystokinin B antagonist and are frequently used as building blocks to create novel peptide or cyclopeptide APIs.[9,10]

Aromatic ammonia-lyases and 2,3-aminomutases comprise a useful and rapidly expanding toolbox of organic synthesis to create enantiopure unnatural α- and β-amino acids.[11]

All these enzymes contain the 3,5-dihydro-5-methylidene-4*H*-imidazol-4-one (MIO) prosthetic group[12,13,14] and play important roles in the metabolism of aromatic amino acids in bacteria, fungi, plants, and animals. The aromatic 2,3-aminomutases mediate the essential step of the enantiopure β-amino acid formation from α-amino acid in the secondary metabolite production.[15] Aromatic ammonia-lyases play essential roles in the non-oxidative ammonia elimination of histidine,[16] phenylalanine, and tyrosine,[17] to create the α,β-unsaturated arylacrylates for the biosynthesis of phenylpropanoids or the L-histidine elimination from the blood by animals.

Under natural conditions, the enantiomer selective ammonia elimination is the preferable direction of the aromatic ammonia-lyases. These enzymes were applied to produce enantiopure D-enantiomers of arylalanines by enantiomer selective destruction of the L-enantiomers from their racemates. Contrary, under ammonia rich reaction conditions these enzymes can catalyze the reaction in a reversible manner to create the L-α-amino acid in high enantiomeric purity by the enantiotope selective ammonia addition onto α,β-unsaturated arylacrylates. Due to their broad substrate tolerance, the most often used biocatalysts are the phenylalanine ammonia-lyases from *Rhodotorula glutinis* (*Rg*PAL)[18,19] *Petroselinum crispum* (*Pc*PAL)[20] and *Anabaena variabilis* (*Av*PAL).[21,22,23]

DSM Pharma Chemicals (Netherlands) developed a multi-ton scale two-step chemo-enzymatic process (thermal cyclisation of L-2-chlorophenylalanine produced by a PAL mediated process), replacing a seven-step chemical procedure for production of (*S*)-2,3-dihydro-1*H*-indole-2-carboxylic acid, useful in the synthesis of hypertension drugs such as indolapril and perindopril.[24]

The histidine ammonia-lyase (HAL, EC 4.3.1.3), phenylalanine ammonia-lyase (PAL, EC 4.3.1.24), tyrosine ammonia-lyase (TAL, 4.3.1.23), phenylalanine/tyrosine ammonia-lyase (PTAL, EC 4.3.1.25), and the recently discovered phenylalanine/tyrosine/histidine ammonia-lyase (XAL)[25] have high sequence similarity in the conserved domains containing the tyrosine as catalytic base, the arginine interacting with the carboxylic group of substrate and the catalytically essential MIO group which is formed usually from an alanine-serine-glycine triad under the assistance of a neighboring tyrosine and asparagine. These two residues are also involved in stabilization of the electrophilic MIO within the catalytic site.[26] While the catalytic machinery performing the substrate binding and deamination within the MIO-enzymes is highly conserved, the aromatic binding pocket of these enzymes is more variable. This part of the catalytic site could be attributed to the differences in the type of enzyme action (lyase vs. mutase activity) and to the

substrate selectivity of natural and unnatural substrates in the MIO-containing aromatic ammonia-lyases and 2,3-aminomutases.[25,27]

Site directed mutational studies revealed that single point mutations in the aromatic binding pocket could increase or decrease the affinity towards the different substrates. The H89F mutation in *Rhodobacter sphareoides* TAL resulted in an enzyme with high PAL activity and decreased TAL activity, whereas the F144H mutant of *Arabidopsis thaliana* PAL achieved TAL activity and have decreased PAL activity.[8,28] Moreover, the steric hindrance within the aromatic binding pocket of *Av*PAL or *Pc*PAL was considerably reduced by rational mutations, providing highly increased enzyme activity towards bulky substrates.[29]

Bioinformatics tools using sequence similarity searches focusing on the highly conserved and the more variable sequence motifs of the MIO-enzyme active site regions allowed identification of novel enzymes with potential unique properties. The motif-based sequence similarity searches and homology modeling were useful tools in identification and characterization of various MIO-enzymes from extremophiles such as the PAL from the thermophilic *Rubrobacter xylanophilus* (*Rx*PAL),[30] PAL from the halophilic marine bacterium *Kangiella koreensis* (*Kk*PAL)[31] and three MIO enzymes from a unique *Pseudomonas fluorescens* strain isolated from a nutrient limited sandstone cave (*Pf*XAL, *Pf*HAL, and *Pf*PAM).[25]

Permanently cold environments on Earth host microorganisms that evolved enzymes with impressive catalytic properties at low temperatures.[32] These enzymes are characterized by high turnover numbers at low to moderate temperatures, by high thermolability at elevated temperatures, and by increased ability to function in organic solvents.[33,34,35,36,37] Cold-adapted enzymes can afford several economic benefits: i) as being more productive than mesophilic or thermophilic homologues at room temperature, they can contribute to energy saving, ii) as being more active at lower temperatures they can reduce the danger of undesirable chemical reactions occurring at higher temperatures, iii) at lower temperatures they are able to convert heat-sensitive substrates, and iv) enzymatic systems can be modulated by rapidly inactivating psychrophilic enzymes with heat.[38]

Pseudozyma antarctica (also known as *Candida antarctica*), first isolated as *Sporobolomyces antarctica* from 9 m depth of Lake Vanda, Antarctica,[39] is a well-known yeast species of the *Pseudozyma* genus. This yeast provided well-studied enzymes from the hydrolase family, most notably lipase A (CaL A) and lipase B (CaL B), with massive industrial use as biocatalysts.[40] These biocatalysts are stable, stereoselective, and well-applicable in hydrolase-catalyzed biotransformations such as hydrolysis, esterification, and transesterification reactions.[41,42,43]

Based on the above considerations, our aim in this study was to find enzymes of PAL or PAM activity from psychrophilic organisms with a special focus on the industrially relevant *Pseudozyma antarctica* yeast species. The heterologous expression of the potential candidate(s) would enable the characterization of the new enzyme(s) (their ammonia-lyase and/or 2,3-aminomutases activity, kinetic parameters, stability issues, etc.), but also the investigation of their biocatalytic ability in the synthesis of variously substituted L- and D-α/β-arylalanines. Moreover, homology models of the new candidates should provide a valuable assistance in establishing the correlation between structure and catalytic activity of the novel biocatalyst(s).

2. Material and methods

2.1 Identification of the PzaPAL gene

The *Pseudozyma antarctica* PAL gene (*Pza*PAL, M9M0D4) was identified in the NCBI database with blastp searches with specified MIO sequence fragments. The UniProt Align tool was used for sequence analysis and comparison to other aromatic ammonia-lyase and 2,3-aminomutase

sequences [*Ustilago maydis* PAL (*Um*PAL, Q96V77), *Rubrobacter xylanophilus* PAL (*Rx*PAL, Q1AV79), *Anabaena variabilis* PAL (*Av*PAL, Q3M5Z3), *Petroselinum crispum* PAL (*Pc*PAL, P24481), *Aradopsis thaliana* PAL (*At*PAL, P35510), *Sorghum bicolor* PAL (*Sb*PAL, C5XXT9), *Rhodobacter sphaeroides* TAL (*Rs*TAL, Q3IWB0), *Rhodosporidium toruloides* TAL (*Rt*TAL, P11544), *Pseudomonas fluorescens* XAL (*Pf*XAL, K0W9Y7), *Pseudomonas fluorescens* HAL (*Pf*HAL, K0WDT6), *Pseudomonas putida* HAL (*Pp*HAL, P21310), *Pseudomonas fluorescens* PAM (*Pf*PAM, K0WLD2), *Pantoea agglomerans* PAM (*Pa*PAM, Q84FL5), *Taxus canadensis* PAM (*Tc*PAM, Q6GZ04), *Chondromyces crocatus* TAM (*Cc*TAM, Q0VZ68) and *Streptomyces globisporus* TAM (*Sg*TAM, Q8GMG0)].

2.2. Cloning and amplification of PzaPAL gene

See in ESI Section 3.

2.3. Expression and purification of PzaPAL

See in ESI Section 4 and 5.

2.4. pH optimum of the PzaPAL-catalyzed reaction

Initial activity of the deamination of L-phenylalanine (5 mM) was monitored at 290 nm for 10 min at 30 °C and different pH-values. For pH 7.0 to 9.0 TRIS-buffer (100 mM) was used; measurements at pH 9.5 to 10.5 were conducted in $(NH_4)_2CO_3$ buffer (100 mM). Measurements at pH 6.0, 6.5, 11.0, 11.5, 12.0 were carried out in PB (Phosphate buffer) (100 mM). Buffers were prepared at room temperature.

2.5. Thermal stability of PzaPAL

The thermal stability tests were investigated i) between pH 7.0 and 10.5 (pH 7.0-9.0 in 100 mM TRIS buffer; pH 9.5-10.5 in 100 mM ammonium carbonate buffer); ii) after 48 h incubation at 10, 20, 30, 40, 50 °C in 100 mM TRIS buffer, pH 8.5; iii) in 100 mM TRIS buffer (pH 8.5) implemented with sodium chloride between 50 and 500 mM. The thermal stability of the enzyme was determined by nano-DSF (*Prometheus NT.48, NanoTemper Technologies;* München, Germany). The capillaries were filled with 0.1 mg mL^{-1} *Pza*PAL solution diluted with the required buffer solutions and placed into the capillary tray of the nano-DSF equipment. Melting curves were measured by heating the samples from 20 °C to 95 °C with 1 °C min^{-1}. The evaluation was executed on the base of the first derivative of the fluorescent signal.

2.6. Kinetic characterization of PzaPAL-catalyzed ammonia elimination reactions

The reaction mixtures contained 100 mM TRIS buffer, pH 8.5, and different concentrations of substrates ((*S*)-**1a**, *rac*-**1b**-**g**, **k**) and were incubated at 30 or 42°C (in case of (*S*)-**1a**) for 3 min. The reactions were started by the addition of purified *Pza*PAL (10 μg mL^{-1} for *rac*-**1a-d**,**f**,**k** and 50 μg mL^{-1} for *rac*-**1e**,**g** in final concentration) in a final volume of 0.2 mL. The measurements were performed in triplicates.

The values of V_{max} and K_M were obtained from non-linear regression fitting of the Michaelis-Menten curves by *Statistica 13.4* using the equation $V = V_{max} \times [S]/(K_M + [S])$ (Figures S9-S25 in ESI). The k_{cat} values were calculated according to equation $k_{cat} = V_{max}/[E_o]$, where $[E_o]$ represents the enzyme concentration used in the kinetic assay. The velocity for each substrate concentration was measured in triplicate.

*2.7. Biotransformation of racemic phenylalanine derivatives (rac-**1a-s**) catalyzed by PzaPAL and PcPAL*

The ammonia elimination reaction mixtures containing 5 mM of the racemic phenylalanines (*rac*-**1a-s**) in 100 mM TRIS buffer (pH 8.5) and purified *Pza*PAL or *Pc*PAL (50 μg, either) in 1 mL reaction volume were incubated at 30 °C. Samples (50 μL) taken at different time points (17, 40, 64, and 168 h) from the reaction mixtures were analyzed by HPLC for conversion and *ee* values, using previously developed methods.[44]
The ammonia addition and elimination reactions were followed by HPLC measurements. Conversions were determined on Agilent 1200 HPLC instrument using Phenomenex Gemini NX-C-18 column and a mixture of NH_4OH buffer (0.1 M, pH 8.5) and MeOH at a flow rate of 1 mL min^{-1}. Conversions were calculated from peak area integrations with use of appropriate response factor (Table S2). Enantiomer separations were carried out on Agilent 1100 HPLC instrument using Crownpak CR-I (+) column and a mixture of aqueous $HClO_4$, pH 1.5 and acetonitrile as eluent at a flow rate of 0.4 mL min^{-1}. (Table S3).

*2.8. Biotransformation of (E)-cinnamic acid derivatives (**2a-s**) catalyzed by PzaPAL and PcPAL*

The reaction mixtures containing substituted (*E*)-cinnamic acids (**2a-s**, 5 mM) in $NH_2CO_2NH_4$ (3M, pH 9.1) supplemented with *Pza*PAL (50 μg mL^{-1}) or in NH_3 (6M, pH 10) supplemented with *Pc*PAL (50 μg mL^{-1}) were incubated at 30 °C. Samples (50 μL) taken at different time points (17, 40, 64, and 168 h) from the reaction mixtures were quenched by adding an equal volume of MeOH, vortexed and centrifuged (13000 rpm, 2 min). The supernatant was transferred to a 0.22 μm filter and used directly for HPLC analysis to determine conversion and *ee* values.

2.9. Homology modeling and simulation of enzyme-substrate interactions

*Pza*PAL initial homology models were created according to our previously published protocol.[45] The initial 8 homology models were subjected to structure superposition, clustering, and a brief CG minimization to yield an average cluster model with MODELLER.[46]This model was completed and adjusted corresponding to the assay conditions of the kinetics characterization of ammonia elimination (100 mM TRIS buffer, pH 8.5). Protein Preparation Wizard[47,48] of Maestro[49] was used in two steps: i) hydrogen atoms were added and bond orders were assigned, and ii) the hydrogen bond network, tautomeric states, side chain conformations of selected amino acids, and ionization states were determined and optimized (pH=8.5). In all four active centers, Tyr91 was set deprotonated and Tyr361 protonated. The L-phenylalanine was docked in the active center of chain A similarly to our previously published induced-fit, covalent docking protocol.[50] Leu115, Leu262, Leu265, Met118, Gln119 of chain A and Ile472, and Lys468 of chain C were mutated to alanine, the MIO group was mutated to alanine and glycine. The L-phenylalanine was docked in a 27×27×27 $Å^3$ grid, centered between the phenolic oxygen of Tyr91 and the exocyclic methylene carbon of the MIO prosthetic group using Glide.[51] Then, all side chains and the MIO group were restored. A covalent bond was created between the amino group of the substrate L-phenylalanine and the exocyclic carbon of MIO. The ligands and the residues in close proximity were minimized, and finally, redundant conformations were eliminated with MacroModel.[52] After this step, side chain conformations of the previously restored residues (except for Lys468 of chain C and the MIO group) were predicted with Prime[53] (with C_α-C_β vectoring, vacuum, 2 steps).
Next, water molecules in the active center and its immediate vicinity were predicted and placed with grand canonical Monte Carlo simulation with the following parameters using Desmond,[54]

[T=303K; 20×20×20 $Å^3$ box size] Simulations were carried out 15 times in parallel (with different random seeds), 500.000 number of passes were used for each simulation, and the final waters were determined upon the most frequent number and configuration of water molecules of the last 10.000 passes.
The final model was minimized with Prime[53] [RMSG: 0.5 kcal mol^{-1} $Å^{-1}$, algorithm: BFGS, implicit water solvation model: VSGB).
This structure was simulated with Desmond in an orthorhombic cell. The box was solvated with TIP3P waters, neutralized with protonated Tris and augmented with 0.072 M Tris, 0.028 M protonated Tris and chloride anion (calculated with a pKa of 8.1). The system was then equilibrated for i) 100 ps with Brownian dynamics at 10K, NVT ensemble; ii) 12 ps with molecular dynamics at 10 K, NVT ensemble; iii) 12 ps with molecular dynamics at 10 K, NPT ensemble, and iv) 12 and 24 ps with molecular dynamics at 303K, NPT ensemble. Harmonic restraints (50 kcal $mol^{-1}Å^{-1}$) were applied to protein heavy atom positions in all steps. The OPLS3e force field was applied in all molecular mechanics calculations and simulations.
Panels of Figure 3 were created with Maestro[49] and Pymol[55].

3. Results and discussion

To our satisfaction, the sequence similarity search allowed the identification of a sequence in the *Pseudozyma antarctica* genome[56] using the highly conserved and the more variable sequence motifs of the MIO-enzyme active site regions [sequence portions of the phenylalanine 2,3-aminomutase of *Taxus canadensis* (*Tc*PAM) and parsley PAL (*Pc*PAL)] against translated nucleotide sequences of yeasts resembling to the MIO-enzymes (UniProt ID: M9M0D4). Since *P. antarctica* is a well-known yeast isolated from cold environment and producing industrially highly important lipases, the PAL of this yeast has been selected as target of the present study. After its identification, the nucleotide sequence of the phenylalanine ammonia-lyase *Pseudozyma antarctica* (*Pza*PAL) gene was optimized for the *E. coli* codon usage. The reoptimized synthetic gene of *Pza*PAL was overexpressed in *E. coli* using a proper production vector coding the His-tagged *Pza*PAL protein. In this study the enzymatic properties and biocatalytic applicability of *Pza*PAL (Scheme 1) were investigated. First, kinetic resolution of racemic substituted phenylalanines **1a-s** by the enzymatic ammonia elimination was studied leading to substituted cinnamic acids and to the residual (*R*)-phenylalanines. Then, the *Pza*PAL-catalyzed enantiotope selective ammonia addition to substituted cinnamic acids **2a-s** was studied leading to the corresponding L-amino acids in high enantiopurity.

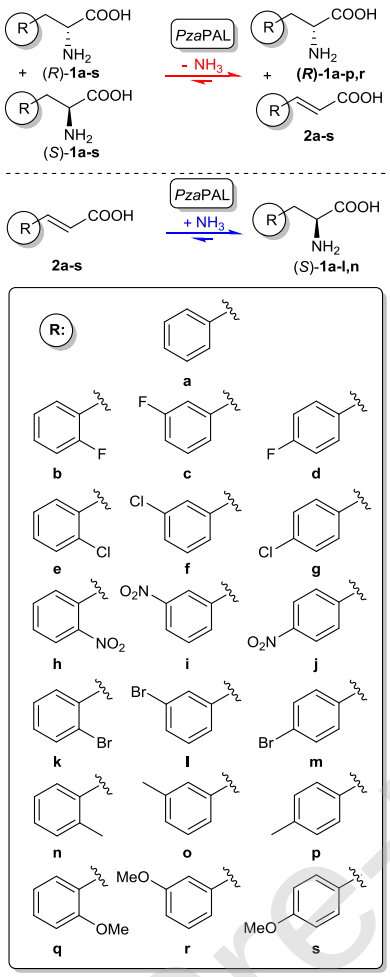

Scheme 1. Substrates and products in *Pza*PAL-catalyzed kinetic resolution of substituted racemic arylalanines *rac*-**1a-s** and enantiotope selective ammonia addition onto (*E*)-arylacrylates **2a-s**

3.1. Identification of the MIO-containing phenylalanine ammonia-lyase from Pseudozyma antarctica (PzaPAL)

The *Pza*PAL gene was identified by BLAST screening yeast genes in the UniProt[57] and GeneBank[58] databases against sequence portions of the aromatic binding pocket of *Tc*PAM and *Pc*PAL, since variations in the substrate affinity of MIO enzymes is modulated mostly by the interactions of the substrate molecule with the amino acid side chains of the aromatic binding region (Figure 1).

The *Pza*PAL has an extra loop with 26 amino acids connected to the aromatic binding pocket containing a -QMQQ- motif of in place of the -xFLx- motif usually present in other PALs which is not typical for the most of MIO enzymes (Figure 1). This -QMQQ- motif and the extra loop region of similar length could be identified only in sequences of closely related fungal PALs of *Ustilago maydis* (*Um*PAL)[59] or *Ustilago hordei* (*Uh*PAL).[60] The three glutamines within the aromatic binding pocket of *Pza*PAL can establish more polar interactions with substituted arylalanines than the conventional PALs with less polar motifs such as -RFLG- in *Rx*PAL, -WFLK- in *Av*PAL, -RFLN- in *Pc*PAL and *At*PAL. The -QMQQ- motif differs significantly from the moderately polar motifs of -HHLA- in *Rs*TAL, -RHLN- in *Sb*PAL, -EHQL- in *Rt*TAL; also, from the -TFHG- motif in *Pf*XAL or from the -LSHA- motif in *Pf*HAL and *Pp*HAL. The extra loop with 26 amino acids following the aromatic binding pocket motif in *Pza*PAL is not typical for most of the MIO enzymes. The *Rt*TAL contains also an extra loop but only with 14 amino

acids, while *Pc*PAL, *At*PAL and *Tc*PAM contains even shorter extra loops. The extra loop is not present in MIO-enzymes of prokaryotes.

The presence of the highly conserved catalytic tyrosine base at the position 91 in *Pza*PAL is consistent with the other MIO enzymes (Figure 2). The highly conserved amino acid triad ASG forming MIO is also present in *Pza*PAL and most of the MIO-enzymes (except the bacterial PAMs having a TSG triad as precursor of the MIO catalytic group). The MIO group stabilizing residues (N266 and Y361) and the substrate carboxylic acid binding arginine (R364) is also highly conserved in *Pza*PAL and in other MIO enzymes (Figure 2).

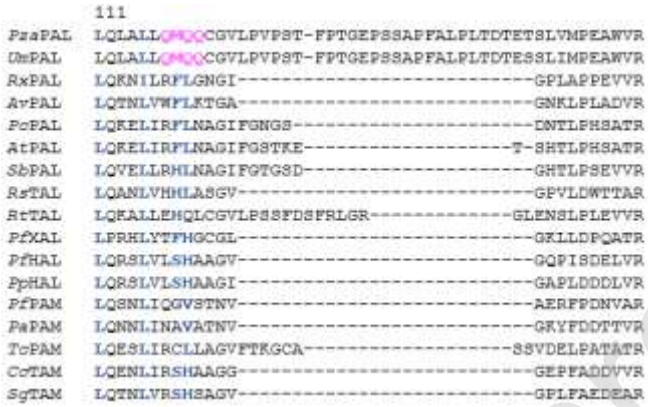

Figure 1. Sequence alignment of the aromatic binding pocket region including an extended loop in various MIO-enzymes [*Pseudozyma antarcti*ca PAL (*Pza*PAL), *Ustilago maydis* PAL (*Um*PAL), *Rubrobacter xilanophilus* PAL (*Rx*PAL), *Anabaena variabilis* PAL (*Av*PAL), *Petroselinum crispum* PAL (*Pc*PAL), *Arbidopsis thaliana* PAL (*At*PAL), *Sorghum bicolor* PAL (*Sb*PAL), *Rhodobacter spheroides* TAL (*Rs*TAL), *Rhodosporidum toruloides* TAL (*Rt*TAL), *Pseudomonas fluorescens* XAL (*Pf*XAL), *Pseudomonas fluorescens* HAL (*Pf*HAL), *Pseudomonas putida* HAL (*Pp*HAL), *Pseudomonas fluorescens* PAM (*Pf*PAM), *Pantenoa agglomerans* PAM (*Pa*PAM), *Taxus canadensis* PAM (*Tc*PAM), *Chondromyces crocatus* TAM (*Cc*TAM) and *Streptomyces globisporus* TAM (*Sg*TAM)] – color codes: pink - the aromatic pocket motif of *Pza*PAL; blue: important amino acids in the aromatic binding pocket of other MIO-enzymes.

Figure 2. Sequence alignment of the highly conserved catalytic domains in various MIO-enzymes. Sequence alignment from by the presented MIO-enzymes. Color codes: red – catalytically essential tyrosine; orange – the MIO forming amino acid triad; green – amino acids stabilizing MIO group; yellow – arginine responsible for binding the carboxylic group of substrate; purple – amino acids related to the (*S*)-PAM activity.

3.2. Homology model of PzaPAL

The detailed homology model of *Pza*PAL was created with our previously published[45] and updated protocol. Since the point mutation of a surface exposed cysteine into serine in the *C*-terminal part did not decrease the catalytic activity of *Pc*PAL, but decreased the aggregation ability of the enzyme expressed in *E. coli*,[61] we followed a similar strategy in this study as well. The homology model of *Pza*PAL showed a surface exposed cysteine at the position 655 which presumably does not have influence on the catalytic activity but contributes to the aggregation ability of the homotetrameric enzyme. Thus, the point mutation of this cysteine into serine (C655S) was introduced to the synthetic gene of *Pza*PAL to reduce the opportunity of enzyme aggregation.

The homology model including simulated structural waters revealed the three conserved water molecules in close proximity to the MIO which were also present in the structures of other PALs (Figure 3, panel A, HOH1-3). However, the *Pza*PAL homology model predicted an additional water molecule in the active center, being atypical for PALs (Figure 3, panel A, HOH4). This water establishes four hydrogen bonds with neighboring residues HOH3, Ser201, Gly467, and with the also atypical Gln119 which belongs to the -QMQQ- motif. This water can play an important role in the orientation of Gln119 pointing the amide carbonyl oxygen towards the aromatic ring of the substrate. The excess negative charge on this carbonyl oxygen can decrease the electron withdrawing (EW) effect of EW substituents at position 4 of the aromatic ring in substituted phenylalanines.

The homology model predicts a possible function of the extended loop with the 26 extra amino acids [loop1, residues 121-150]. The loop1 in two of the four of peptide chains of the homotetrameric *Pza*PAL establishes interactions with each other (Figure 3, panel C). Moreover, another shorter loop [loop2, residues 226-237] is involved in the local loop network (Figure 3, panel B). Since loop1 is directly connected to the -QMQQ- motif of the aromatic binding pocket (Figure 3, panel B and C), it can be assumed that this interacting loop network is responsible for allosteric modulation of adjacent active sites within the tetrameric *Pza*PAL during substrate transformation.

3.3. Cloning and expression of PzaPAL

The *Pza*PAL gene was codon optimized for the *E. coli* codon usage and synthetized in pUC57 vector. The gene was inserted in to pET-19b expression vector with NdeI and BamHI restriction endonucleases to encode the *N*-terminal His_{10}-tagged form of the *Pza*PAL. The transformed *E. coli* Rosetta (DE3)pLysS cells with pET-19b_*Pza*PAL expression vector were grown in LB medium supplemented with carbenicillin and chloramphenicol at 37 °C, and *Pza*PAL expression was induced with addition of IPTG at 25 °C. Purification of the His-tagged *Pza*PAL was performed with Ni-NTA agarose affinity chromatography.

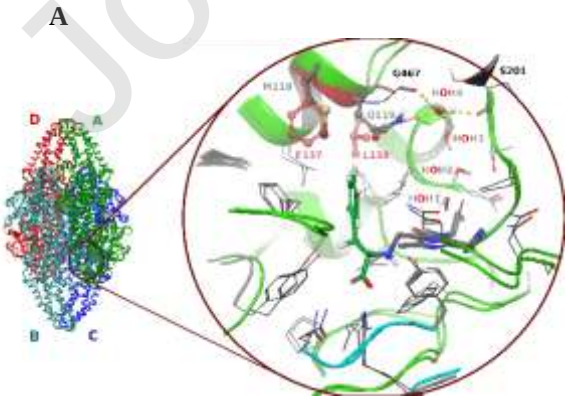

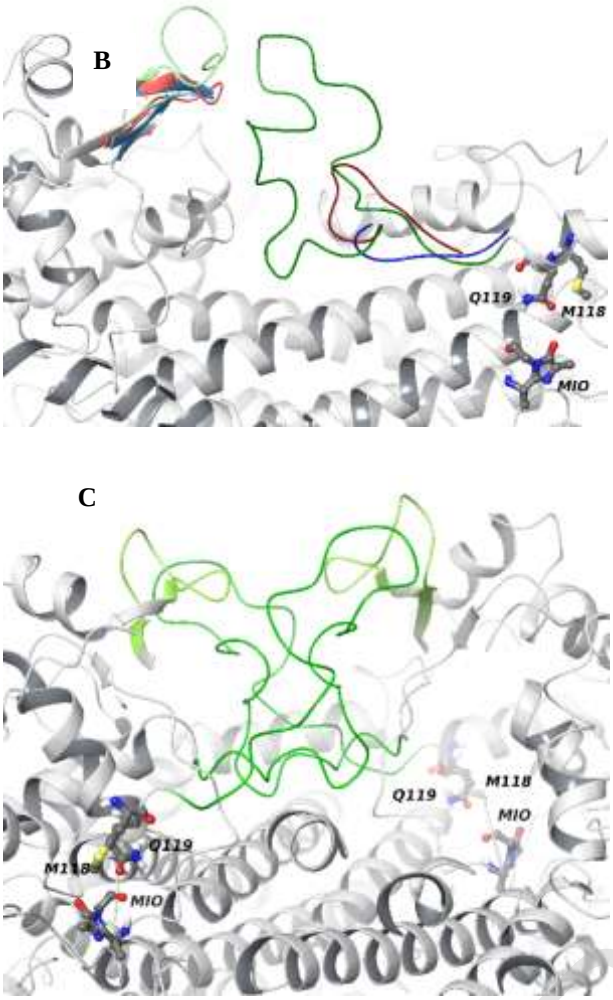

Figure 3. The catalytic site (A) and the extended loops (B, C) in the structure of tetrameric *Pza*PAL (A) predicted by homology modeling. [Panel **A**: overlay of the active centers of *Pza*PAL and *Pc*PAL displaying identical residues next to the substrate and three identically positioned waters HOH1-3 by sticks representation and the main differences in the two active sites M118/F137, Q119/L138, HOH4 (*Pza*PAL/*Pc*PAL, respectively) by ball and stick representation. HOH4 interactions are displayed with S201 and G467. Panel **B**: chains A and C of the homology model displaying the extended loops of *Pza*PAL (loop 121-150 in dark green, loop 226-237 in light green) compared to the corresponding shorter loops of *Pc*PAL (loop 141-150 in dark red, loop 223-232 in light red) and even shorter loops of *Av*PAL (loop 189-198 in dark blue, loop 109-115 in light blue). Panel **C**: the extensive interactions of the extended loops 121-150 and 226-237 within the tetramer of *Pza*PAL].

3.4. pH optimum of the PzaPAL-catalyzed elimination reaction

The effect of the pH on the ammonia-lyase activity of *Pza*PAL with L-phenylalanine was investigated between 6.0 and 12.0 (Figure 4). The maximum activity was observed at pH 8.5 which is similar to *Uh*PAL (pH 8.8)[60] and *Um*PAL (pH 8.8-9.2).[59] Differential thermal calorimetric measurements indicated that the *Pza*PAL enzyme retained its thermal stability in a broad pH range from 7.0 to 10.5, while at higher pH values the structural stability of the enzyme decreased considerably (Figure 5).

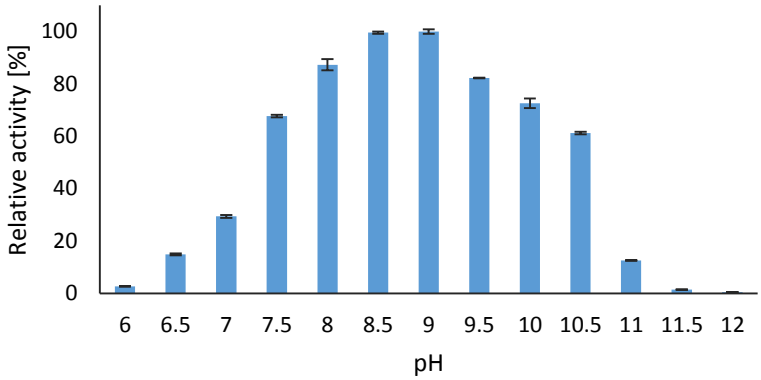

Figure 4. Effect of the pH upon *Pza*PAL activity in presence of L-Phe.

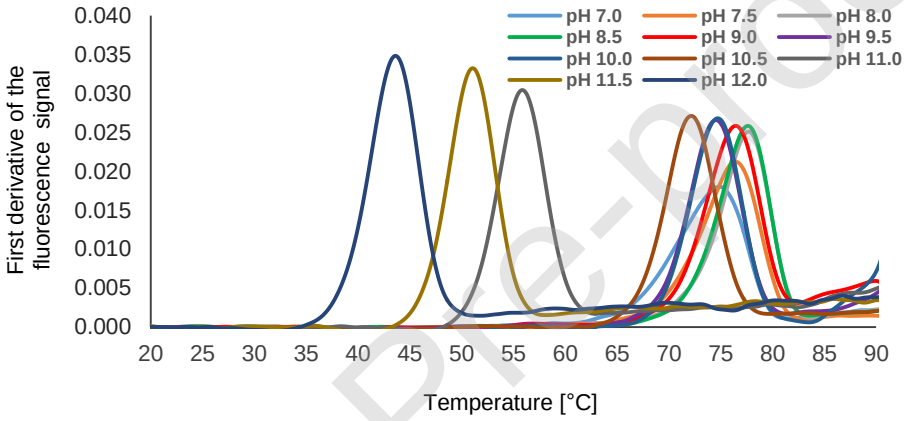

Figure 5. Thermal unfolding curves of *Pza*PAL at different pH values by nano-DSF measurements.

3.5. Thermal behavior of PzaPAL

The effect of temperature on enzyme activity of *Pza*PAL (without prior incubation) was assayed at different temperatures ranging from 5-60 °C at the optimal pH value. A strong temperature dependence of the enzyme activity with temperature was detected, displaying highest value at 45 °C (Figure 6). However, it is worth mentioning that despite of the psychrophilic origin of *Pza*PAL, the high melting temperature (77.5 °C) of the enzyme was found to be superior compared to most of other known PALs (see ESI 1.12 and 1.14).

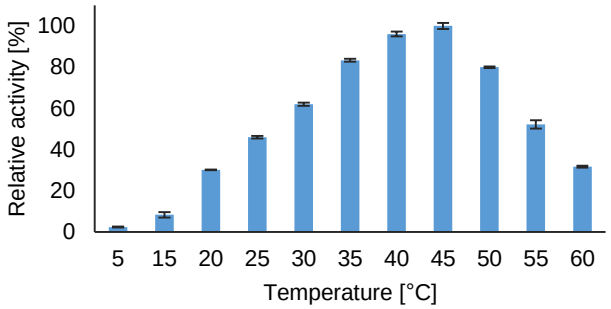

Figure 6. Temperature effect upon *Pza*PAL activity using L-Phe as substrate (without preincubation).

*Pza*PAL was also pre-incubated at different temperatures in the range of 10-50 °C, at the optimal pH value for 24 h and assayed afterwards. The results (Figure S3 in ESI) showed that in the range of 10-40 °C after 8 h preincubation the enzyme retained more than 90% of its original activity. Considerable activity decrease was observed after 24 h preincubation at 40 and 50 °C. This was in good agreement with the behavior of *Uh*PAL remaining active after 10 min incubation at 50 °C but inactivating at 60 °C and 70 °C.[60]

The enzyme was pre-incubated also in 6M NH_3, pH 10.0 (adjusted by bubbling CO_2) at different temperatures ranging from 10-50 °C for 24 h and assayed afterwards. The *Pza*PAL inactivated rapidly in 6M NH_3, after 24 h only the enzyme incubated at 10 °C exhibited some residual activity, while in 0.1M TRIS-buffer the enzyme activity was well preserved (Figure S5 in ESI).

3.6. Effect of salt concentration on the activity of PzaPAL in the elimination from L-Phe

Various NaCl concentrations were studied for their impact on *Pza*PAL activity at pH 8.5. As NaCl concentration was increased from 0 to 500 mM, the activity decreased monotonously (Figure S6 in ESI). According to this analysis, the enzyme presented the maximal thermal stability in the absence of NaCl, therefore no salt was used in the buffer solutions (Figure S7 and Table S9 in ESI).

3.7. Kinetic characterization and substrate scope of the PzaPAL-catalyzed ammonia elimination

Besides with L-Phe [(*S*)-**1a**], the kinetics of ammonia elimination by *Pza*PAL was characterized with several racemic phenylalanine derivatives *rac*-**1a-g,k** (Table 1). The non-conventional aromatic binding pocket of the *Pza*PAL enzyme, compared to other PALs, resulted in significant differences in the catalytic activity and substrate affinity (Table 1).

The K_M value of L-phenylalanine (*S*)-**1a** with *Pza*PAL (K_M= 0.83 mM) was similar to those found with the closely related *Uh*PAL (K_M= 0.45 mM)[60] and *Um*PAL (K_M= 1.05 mM),[59] one order of magnitude higher than with *Pc*PAL (K_M= 0.083 mM),[50] *Av*PAL (K_M= 0.06 mM),[62] *At*PAL1 (K_M = 0.068 mM),[63] but smaller than with *Pf*XAL (K_M= 2.6 mM).[25] *Pza*PAL had an about two times higher turnover number (k_{cat}= 2.97 s^{-1}) than *Pc*PAL (k_{cat}= 1.38 s^{-1}). This turnover value was similar to that of *Pf*XAL (k_{cat}= 2.38 s^{-1})[25] and somewhat lower than of *Av*PAL (k_{cat}= 4.3 s^{-1}).[62] Temperature-dependent kinetics of *Pza*PAL were studied with L-phenylalanine (*S*)-**1a** at 30°C (Figure S8 in ESI) and 42°C (Figure S9 in ESI) showing weakly decreasing K_M values ($K_{M(30°C)}$= 0.8 mM; $K_{M(42°C)}$= 1.1 mM) with significantly increasing turnover numbers ($k_{cat(30°C)}$= 2.97 s^{-1}; $k_{cat(42°C)}$= 8.2 s^{-1}).

Table 1. Kinetic parameters of *Pza*PAL and *Pc*PAL in ammonia elimination reactions of several phenylalanine derivatives.

Substrate	*Pza*PAL		*Pc*PAL	
	K_M [mM]	k_{cat} [s^{-1}]	K_M [mM]	k_{cat} [s^{-1}]
(*S*)-**1a** (Ph)	0.83	2.94	0.055	1.38
rac-**1b** (*o*-F)	2.33	4.48	0.079	1.01
rac-**1c** (*m*-F)	1.13	8.00	0.147	0.96
rac-**1d** (*p*-F)	1.69	4.22	0.024	0.41
rac-**1e** (*o*-Cl)	>2.82[a]	1.03[b]	0.083	0.95
rac-**1f** (*m*-Cl)	1.45	1.92	0.041	0.96
rac-**1g** (*p*-Cl)	>10.8[a]	0.26[b]	0.033	0.55
rac-**1k** (*o*-Br)	>2.62[a]	0.69[b]	0.068	0.88

[a] The K_M value could not be determined exactly because at high substrate concentration the *Pza*PAL-catalyzed reaction did not approach V_{max}. [b] The k_{cat} parameter was determined at the highest achievable substrate concentration of the kinetics study with different enzyme concentrations.

Kinetics investigations of *Av*PAL with *rac*-**1b** (K_M= 0.75 mM, k_{cat}= 1.1 s^{-1}) and with *rac*-**1d** (K_M= 0.56 mM, k_{cat}= 1.06 s^{-1}) were also performed.[23] The K_M values *Av*PAL for the *o*- and *p*-fluorophenylalanines *rac*-**1b,d** were 2-3 times smaller than for *Pza*PAL, but *Pza*PAL had 3-4 times higher turnover values with these substrates as *Av*PAL.

The comparative kinetic studies with *Pza*PAL and *Pc*PAL using racemic substituted phenylalanines *rac*-**1b-g**,**k** revealed that the saturated rate (V_{max}) was not achievable with *rac*-**1e**,**g**,**k** in the investigated substrate concentration range due to the limited solubility of the unnatural amino acids. Therefore, only the k_{cat} values were determined at the highest achievable substrate concentration with different enzyme concentrations (Figures S13, S15, S16 in ESI). The fluoro- (*rac*-**1b-d**), chloro- (*rac*-**1e-g**) and *o*-bromo- (*rac*-**1k**) phenylalanines had also higher K_M values with *Pza*PAL than with *Pc*PAL, but again the turnover values with *Pza*PAL are higher than with *Pc*PAL. Presumably, the completely different and more polar amino acids in the aromatic binding pocket of *Pza*PAL could cause this increase of turnover values compared to the "conventional" PALs.

In addition to L-phenylalanine (*S*)-**1a**, *Pza*PAL was tested with several further natural amino acids for ammonia elimination reaction. L-Tyr was found to be a quite poor substrate for *Pza*PAL (1 % relative activity compared to that with L-Phe), similar to *Uh*PAL[60] and *Um*PAL[59] which were reported having no reaction with L-Tyr. Furthermore, *Pza*PAL did not catalyze the ammonia elimination from L-His, L-Trp, L-Asp, L-Asn or L-Gln.

*3.8. Kinetic resolution of rac-phenylalanine derivatives (rac-**1a-s**) mediated by PzaPAL*

The biocatalytic properties of *Pza*PAL were investigated first by kinetic resolution of *rac*-**1a-s** using the ammonia elimination reactions. The biocatalytic performance of *Pza*PAL was compared to the already well-characterized PAL from parsley (*Pc*PAL) (Table 2).

High enantiomer selectivity was observed in most of the *Pza*PAL-catalyzed kinetic resolutions (plain typed values in Table 2, with conversion values within 3% deviation for the calculated full selectivity case) except the ammonia elimination from the racemic *o*-nitro- (*rac*-**1h**), *p*-nitro- (*rac*-

1j), *p*-bromo- (*rac*-**1m**) phenylalanines. In the case of attempted kinetic resolutions with *Pza*PAL using phenylalanines substituted with electron-donating groups (*o*-, *m*-, or *p*-methyl: *rac*-**1n-o**; *o*-, *m*-, or *p*-methoxy: *rac*-**1q-s**) reactions proceeded with moderate, low or even negligible conversion (no product was detected with *o*- and *p*-methoxyphenylalanines *rac*-**1q,s**) but with perfect enantiomer selectivity (for *rac*-**1n-p,r**).

Table 2. Kinetic resolution of racemic phenylalanine derivatives (*rac*-**1a-s**) catalyzed by *Pza*PAL (as compared to by *Pc*PAL).

	after 17 h		after 168 h	
Subst.	*Pza*PAL Conv.[a] ($ee_{(R)\text{-}\mathbf{1a\text{-}s}}$) [%]	*Pc*PAL Conv.[a] ($ee_{(R)\text{-}\mathbf{1a\text{-}s}}$) [%]	*Pza*PAL Conv.[a] ($ee_{(R)\text{-}\mathbf{1a\text{-}s}}$) [%]	*Pc*PAL Conv.[a] ($ee_{(R)\text{-}\mathbf{1a\text{-}s}}$) [%]
rac-**1a** (Ph)	49 (>99)	49 (>99)	49 (>99)	**54** (>99)
rac-**1b** (*o*-F)	49 (>99)	52 (>99)	53 (>99)	**69** (>99)
rac-**1c** (*m*-F)	49 (>99)	52 (>99)	52 (>99)	**63** (>99)
rac-**1d** (*p*-F)	51 (>99)	**54** (>99)	51 (>99)	**59** (>99)
rac-**1e** (*o*-Cl)	48 (98)	49 (>99)	50 (>99)	**64** (>99)
rac-**1f** (*m*-Cl)	47 (88)	51 (>99)	50 (>99)	**61** (>99)
rac-**1g** (*p*-Cl)	44 (82)	**53** (>99)	50 (>99)	**64** (>99)
rac-**1h** (*o*-NO_2)	**35** (43)	**67** (>99)	**62** (>99)	**82** (>99)
rac-**1i** (*m*-NO_2)	21 (26)	**63** (>99)	40 (64)	**91** (>99)
rac-**1j** (*p*-NO_2)	**56** (88)	**96** (>99)	**78** (94)	**99**[b] ([c])
rac-**1k** (*o*-Br)	43 (79)	49 (>99)	49 (99)	**58** (>99)
rac-**1l** (*m*-Br)	29 (39)	50 (>99)	47 (87)	**60** (>99)
rac-**1m** (*p*-Br)	**18** (17)	50 (>99)	38 (58)	**53** (>99)
rac-**1n** (*o*-CH_3)	50 (>99)	49 (>99)	50 (>99)	**52** (>99)
rac-**1o** (*m*-CH_3)	10 (12)	29 (45)	18 (23)	48 (>99)
rac-**1p** (*p*-CH_3)	1 ([c])	47 (94)	6 (7)	48 (>99)
rac-**1q** (*o*-CH_3O)	0 ([c])	**7** (6)	0 ([c])	**25** (30)
rac-**1r** (*m*-CH_3O)	20 (25)	48 (>99)	35 (53)	51 (>99)
rac-**1s** (*p*-CH_3O)	0 ([c])	**22** (25)	0 ([c])	**37** (57)

[a] Conversions were determined by HPLC on C-18 reversed phase. Conversion values in plain: high enantiomer selectivity, conversion values in underscored bold: low enantiomer selectivity due to partial consumption of the (*R*)-enantiomer. [b] Both enantiomers were consumed. [c] Not determined.

*3.9. The PzaPAL-catalyzed ammonia addition reaction onto cinnamic acid derivatives **2a-s***

Addition reactions with various PALs were typically performed in 5-6M NH_3, pH 10 (adjusted by bubbling CO_2) at 30 °C or 37 °C.[11] Herein, we investigated the optimal reaction conditions for *Pza*PAL in the enantiotope selective ammonia addition reaction, including the temperature, the optimal pH, the effect of the ammonia source and concentration.

*3.10. Temperature effect on the ammonia addition reaction onto **2a** by PzaPAL*

Because *Pza*PAL originated from *Pseudozyma antarctica*, a yeast first isolated from cold Antarctic environment,[39] we also investigated the effect of the temperature on the amination reaction of (*E*)- cinnamic acid. The activity of *Pza*PAL pre-incubated in 6M NH_3 at different temperatures (10-50 °C: Figure S5 in ESI) decreased rapidly with increasing temperature (negligible residual activity of *Pza*PAL was observed after 1 h preincubation at 40 or 50 °C). Therefore, the detailed temperature effect study on the addition reaction was performed in the range of 10-30 °C (Table S10 in ESI) indicating maximal activity at 30 °C. Consequently, all further addition reactions were performed at 30 °C.

*3.11. Effect of pH on the ammonia addition reaction onto **2a** by PzaPAL*

One of the most important factors influencing enzyme activity is the pH. Therefore, the effect of pH on the ammonia addition reaction was also investigated using 6M NH_3 solution in the range pH 9.1–10.0 (adjusted by bubbling CO_2). Buffering the reaction to lower pH values of the NH_3-containing medium was beneficial and the *Pza*PAL-catalyzed conversion of (*E*)-cinnamic acid **2a** to L-phenylalanine (*S*)-**1a** was maximal at pH 9.1 (Table S11 in ESI). It was not possible to test NH_3 buffer solutions of 6M at pH values under 9.1.

*3.12. Effect of the ammonia source and concentration on the ammonia addition reaction onto **2a** by PzaPAL*

The concentration of ammonia has a significant effect on the rate of reaction and position of equilibrium. In order to achieve good conversions, 5-6M ammonia is typically used in the PAL-catalyzed ammonia addition reactions.[11] The effect of different ammonia sources on *Pza*PAL-catalyzed (*E*)-cinnamic acid **2a** amination was investigated using purified enzyme at the optimal pH (9.1) in 0.5-5M NH_3 and in 0.5-4M $NH_2CO_2NH_4$ buffers, respectively. It was shown that in both buffers the reaction was fully enantiotope selective providing the product (*S*)-**1a** in enantiomeric excess exceeding 99%. The conversion (and its rate) was significantly lower at 0.5M concentration of ammonia than at 3-5M (Table 3 and S12 in ESI). The highest conversion of amination could be achieved using ammonium carbamate as an ammonia source at a concentration of 3M. Therefore, 3M $NH_2CO_2NH_4$ was selected as the ammonia source for the further investigations on ammonia addition onto substituted (*E*)-cinnamic acids **2a-s** (Table 4).

Table 3. Biotransformation of (*E*)-cinnamic acid (**2a**) catalyzed by *Pza*PAL at different concentrations of $NH_2CO_2NH_4$ buffer.

Buffer conc. [M]	**Conversion in $NH_2CO_2NH_4$ [%]**			
	4 h	20 h	43 h	67 h
0.5	18	34	33	35
1	20	48	54	53
2	17	52	70	71
3	16	52	79	83
4	11	32	68	82

*3.13. The substrate scope of PzaPAL-catalyzed enantiotope selective ammonia addition reaction onto cinnamate derivatives **2a-s***

Most of the *o*-substituted (*E*)-cinnamic acids (**2b,e,h,k,n**) were proper substrates in the *Pza*PAL-catalyzed enantiotope selective ammonia addition, with the exception of (*E*)-*o*-methoxy-cinnamic acid **2q** which was not transformed at all.

Table 4. Enantiotope selective ammonia addition onto (*E*)-arylacrylates (**2a-s**) catalyzed by *Pza*PAL (as compared to by *Pc*PAL).

	after 17 h		after 168 h	
Substrate	*Pza*PAL Conv. ($ee_{(S)\text{-}\mathbf{1a\text{-}s}}$)[a] [%]	*Pc*PAL Conv. ($ee_{(S)\text{-}\mathbf{1a\text{-}s}}$)[a] [%]	*Pza*PAL Conv. ($ee_{(S)\text{-}\mathbf{1a\text{-}s}}$)[a] [%]	*Pc*PAL Conv. ($ee_{(S)\text{-}\mathbf{1a\text{-}s}}$)[a] [%]
***2*a** (Ph)	41 (>99)	81 (>99)	80 (>99)	81 (**98**)
***2*b** (*o*-F)	94 (>99)	96 (**97**)	96 (>99)	95 (**92**)
***2*c** (*m*-F)	93 (>99)	89 (**97**)	93 (>99)	89 (**97**)
***2*d** (*p*-F)	11 (>99)	78 (>99)	51 (>99)	78 (**98**)
***2*e** (*o*-Cl)	98 (>99)	97 (**94**)	98 (>99)	98 (**70**)
***2*f** (*m*-Cl)	5 (**91**)	93 (**97**)	20 (**96**)	93 (**93**)
***2*g** (*p*-Cl)	3 (>99)	92 (**99**)	9 (>99)	91 (**96**)
***2*h** (*o*-NO_2)	32 (**92**)	98 (**89**)	45 (**92**)	98 (**82**)
***2*i** (*m*-NO_2)	2 (**78**)	80 (**89**)	4 (**89**)	89 (**78**)
***2*j** (*p*-NO_2)	78 (**92**)	97 (**75**)	91 (**92**)	97 (**62**)
***2*k** (*o*-Br)	41 (>99)	97 (>99)	95 (>99)	97 (**95**)
***2*l** (*m*-Br)	1 ([b])	92 (>99)	5 (>99)	93 (**95**)
***2*m** (*p*-Br)	0 ([b])	88 (>99)	1 ([b])	90 (>99)
***2*n** (*o*-CH_3)	27 (>99)	84 (>99)	74 (>99)	84 (**99**)
***2*o** (*m*-CH_3)	0 ([b])	44 (>99)	0 ([b])	74 (**97**)
***2*p** (*p*-CH_3)	0 ([b])	34 (>99)	0 ([b])	55 (>99)
***2*q** (*o*-CH_3O)	0 ([b])	21 (>99)	0 ([b])	49 (>99)
***2*r** (*m*-CH_3O)	0 ([b])	58 (>99)	0 ([b])	71 (>99)
***2*s** (*p*-CH_3O)	0 ([b])	0 ([b])	0 ([b])	0 ([b])

[a] Enantiomeric excess values were determined by HPLC on Crownpak CR-I (+) chiral column. Ee values in plain: perfect enantiotope selectivity (no (*R*)-enantiomer could be detected); Ee values in underscored bold: non-perfect enantiotope selectivity due to formation of the (*R*)-enantiomer. [b] Not determined.

The *Pza*PAL-catalyzed ammonia addition onto substituted (*E*)-cinnamic acids **2a-e,g,k,l,n** yielded the corresponding enantiopure L-phenylalanines (*S*)-**1a-e,g,k,l,n** with variable conversions. Excellent conversions (>90%) were achieved with the *o*-F, *m*-F and *o*-Cl substituted cinnamates **2b,c,e** within 17 h, and with the *o*-Br substituted cinnamate after 168 h. The absent or negligible conversion (<5% within 168 h) observed with substituted (*E*)-cinnamic acids **2i,m,o-s** could be rationalized by the increased negative charge of the aromatic binging pocket due to the partial negative charge on Q119 carbonyl oxygen. The excess negative charge in the aromatic

binding pocket in the neighborhood of the *p*- and *m*-position of the phenyl ring of the substrate (Figure 3A) could enhance the electron donating effect of the methyl (**2n-p**) or methoxy (**2q-s**) substituents present in substituted (*E*)-cinnamic acids.

As the reaction should involve an interaction of the forming amino-MIO intermediate as nucleophile with an electrophilic intermediate forming from the substrate cinnamate, the increasing electron donating effect of the aromatic ring decreases the reactivity in the ammonia addition reaction.

In case of the nitro-substituted (*E*)-cinnamic acids (**2h-j**) more rigid aromatic binding pocket partially hindered the reaction due to steric effects but the more electron rich environment could contribute to the higher degree of enantiotope selectivity of the *Pza*PAL-catalyzed ammonia addition onto nitro-substituted (*E*)-cinnamic acids (**2h-j**) than found with the *Pc*PAL indicated by the higher enantiomeric excess of nitrophenylalanines (*S*)-**1h-j** from the *Pza*PAL-catalyzed reaction after 168 h as compared to the corresponding values from the *Pc*PAL-catalyzed process.

Interestingly, while in many instances the *Pza*PAL-catalyzed process after 168 h reaction time resulted in enantiopure products ($ee_{(S)\text{-}\mathbf{1a\text{-}e,g,k,l,n}}$ >99 %; with the exception of the *m*-chloro-, *o*-, *m*- and *p*-nitro-substituted cinnamates **2f,h,i,j**), the *Pc*PAL-catalyzed ammonia addition provided incomplete enantiotope selectivity onto cinnamates **2b-l** and **2o**.

4. Conclusions

In this study, the properties and biocatalytic applicability of a novel ammonia-lyase from the yeast *Pseudozyma antarctica* were investigated. The *Pza*PAL gene was successfully identified, cloned and expressed in *E. coli* and the forming enzyme was characterized. The *Pza*PAL exhibited maximal activity at pH 8.5, similarly to other characterized PALs. The highest enzyme activity was detected at 45 °C (without prior incubation) while thermal unfolding of the enzyme was observed at 77.5 °C. Long-term stability tests indicated that in the range of 10-40 °C the enzyme retained more than 90% of its initial activity within 8 h. Despite of the lower affinity of phenylalanines (*S*)-**1a** and *rac*-**1b-f** to *Pza*PAL than to PAL from parsley (*Pc*PAL), with *Pza*PAL higher turnover number/catalytic efficiency were observed than with *Pc*PAL.

The significantly different catalytic activity of *Pza*PAL could be attributed to the completely different amino acids in the aromatic binding pocket as compared to *Pc*PAL. The structure of *Pza*PAL predicted by homology modeling showed a local network of extended loops and predicted the presence of an atypical, bound water molecule partly responsible for the orientation of Gln119 enhancing the local negative charge in the aromatic binding region. The *Pza*PAL-catalyzed elimination reactions from racemic phenylalanines with moderately bulky substituents *rac*-**1a-g,k,n** proceeded with high enantiomer selectivity providing at near to 50 % conversion the residual enantiopure phenylalanine (*R*)-**1a-g,k,n**. Elimination from *rac*-**1i**,**m**,**o**,**p**,**r** bearing larger but not extremely charged substituents proceeded with moderate to low conversion, while no product was detected from phenylalanines *rac*-**1q,s** bearing *o*- or *p*-methoxy substituents. While the *Pc*PAL-catalyzed ammonia addition onto **2b-l** and **2o** proceeded with incomplete enantiotopic selectivity, *Pza*PAL yielded from a number of substituted cinnamates **2a-e,g,k,l,n** the enantiopure products ($ee_{(S)\text{-}\mathbf{1a\text{-}e,g,k,l,n}}$ >99%) These properties render *Pza*PAL as catalyst of choice for preparation of a number of substituted (*R*)- or (*S*)-phenylalanines in enantiopure form. Moreover, due to its remarkably different aromatic binding site features, *Pza*PAL is a good initial candidate for biocatalyst engineering with targeted mutations for altered substrate scope leading to further unnatural α-amino acids in high enantiopurity.

Credit author statement

Andrea Varga: Investigation, Methodology, Editing, Writing - Original Draft; Pál Csuka: Investigation, Editing; Orlavanah Sonesouphap: Investigation; Gergely Bánóczi: Software, Visualization; Monica Ioana Toșa: Methodology, Project administration, Formal analysis; Gabriel Katona: Validation, Resources; Zsófia Molnár: Investigation; László Csaba Bencze: Writing - Review & Editing, Supervision; László Poppe: Conceptualization, Writing - Review & Editing, Supervision, Project administration, Funding acquisition; Csaba Paizs: Conceptualization, Methodology, Project administration, Supervision, Writing - Review & Editing.

Declaration of interests

☒ The authors declare that they have no known competing financial interests or personal relationships that could have appeared to influence the work reported in this paper.

Acknowledgements

This work was supported by the project "Entrepreneurship for innovation through doctoral and postdoctoral research", POCU/360/6/13/123886 co-financed by the European Social Fund, through the Operational Program for Human Capital 2014-2020, by project NEMSyB [ID P37_273, Cod MySMIS 103413; funded by National Authority for Scientific Research and Innovation (ANCSI) and co-funded by the European Regional Development Fund, Competitiveness Operational Program 2014-2020 (POC) and by the Swiss National Science Foundation (SNSF) - project PROMYS, grant nr. IZ11Z0_166543. This work was also supported by the Higher Education Excellence Program of the Ministry of Human Capacities (Budapest, Hungary) in the frame of Biotechnology research area of Budapest University of Technology and Economics (BME FIKP-BIO), the National Research, Development and Innovation Fund of Hungary (Budapest, Hungary; project SNN-125637) and by CELSA (BME-KU Leuven, ConSolid project).

References

[1] F. Agostini, J. S. Völler, B. Koksch, G. C. Acevedo-Rocha, V. Kubyshkin, N. Budisa, Angew. Chem. Int. Ed. 56 (2017) 9680–9703.
[2] Biocatalysis: An Industrial Perspective (G. de Gonzalo Calvo, P. Domínguez de Maria, Eds.), RSC Publishing: Cambridge, 2018.
[3] K. Faber, Biotransformations in Organic Chemistry, 7th Ed., Springer: Heildelberg, 2018.
[4] M. Jin, M. A. Fischbach, J. Clardy, J. Am. Chem. Soc. 128 (2006) 10660–10661.
[5] S. D. Christenson, W. Liu, M. D. Toney, B. Shen, J. Am. Chem. Soc. 125 (2003) 6062–6063.
[6] C. L. Steele, Y. Chen, B. A. Dougherty, W. Li, S. Hofstead, K. S. Lam, Z. Xing, S. J. Chiang, Arch. Biochem. Biophys. 438 (2005) 1–10.
[7] K. D. Walker, K. Klettke, T. Akiyama, R. Croteau, J. Biol. Chem. 279 (2004) 53947–53954.
[8] G. V. Louie, M. E. Bowman, M. C. Moffitt, T. J. Baiga, B. S. Moore, J. P. Noel, ChemBiol 13 (2006) 1327–1338.
[9] F. Kudo, A. Miyanaga, T. Eguchi, Nat. Prod. Rep. 31 (2014) 1056–1073.
[10] A. Stevenazzi, M. Marchini, G. Sandrone, B. Vergani, M. Lattanzio, Bioorg. Med. Chem. Lett. 24 (2014) 5349–5353.
[11] F. Parmeggiani, N. J. Weise, S. Ahmed, N. J. Turner, Chem. Rev. 118 (1) (2018) 73–118.
[12] a) L. Poppe, Curr. Opin. Chem. Biol. 2001, 5, 512–524; b) L. Poppe, J. Rétey, Curr. Org. Chem. 7 (2003) 1297–1315.
[13] N. J. Turner, Curr. Opin. Chem. Biol. 15 (2011) 234–240.

[14] L. Poppe, C. Paizs, K. Kovács, F. D. Irimie, B. G. Vértessy, Meth. Mol. Biol. 794 (2012) 3–19.
[15] B. Wu, W. Szymański, M. M. Heberling, B. L. Feringa, D. B. Janssen, Trends Biotechnol. 29 (2011) 352–362.
[16] H. Morrison, C. Bernasconi, G. Pandey, Photochem. Photobiol. 40 (1984) 549–550.
[17] X. Zhang, C. Liu, Mol. Plant 8 (2015) 17–27.
[18] S. Yamada, K. Nabe, N. Izuo, K. Nakamichi, I. Chibata, Appl. Environ. Microbiol. 42 (1981) 773−778.
[19] G. Renard, J.-C. Guilleux, C. Bore, V. Malta-Valette, D. A. Lerner, Biotechnol. Lett. 14 (1992) 673−678.
[20] C. Paizs, A. Katona, J. Rétey, Chem. Eur. J. 12 (2006) 2739−2744.
[21] N. J. Weise, F. Permeggiani, S. T. Ahmed, N. J. Turner, Top. Catal. 61 (2018) 288–295.
[22] S. T. Ahmed, F. Permeggiani, N. J. Weise, S. L. Flitsch, N. J. Turner, Org. Lett. 18 (2016) 5468–5471.
[23] S. L. Lovelock, N. J. Turner, Bioorg. Med. Chem. 22 (2014) 5555−5557.
[24] F. B. J. van Assema, N. Sereinig (DSM): Method for producing optically active phenylalanine compounds from cinnamic acid derivatives employing a phenylalanine ammonia lyase derived from *Idomarina loihiensis*. WO 2008/031578 (2008) and PCT/EP 2007/007945 (2007).
[25] P. Csuka, V. Juhász, S. Kohári, A. Filip, A. Varga, P. Sátorhelyi, L. C. Bencze, H. Barton, C. Paizs, L. Poppe, ChemBioChem, 19 (2017) 1–9.
[26] G. G. Wybenga, W. Szymanski, B. Wu, B. L. Feringa, D. B. Janssen, B. W. Dijkstra, Biochemistry 53 (2014) 3187−3198.
[27] B. Wu, W. Szymanski, G. G. Wybenga, M. M. Heberling, S. Bartsch, S. Wildeman, G. J. Poelarends, B. L. Feringa, B. W. Dijkstra, D. B. Janssen, Angew. Chem. Int. Ed. 51 (2012) 482–486.
[28] K. T. Watts, B. N. Mijts, P. C. Lee, A. J. Manning, C. Schmidt-Dannert, Chem. Biol. 13 (2006) 1317–1326.
[29] a) S. T. Ahmed, F. Parmeggiani, N. J. Weise, S. L. Flitsch and N. J. Turner, ACS Catal. 5 (2015) 5410−5413; b) A. Filip, E. Z. A. Nagy, S. D. Tork, G. Bánóczi, M. I. Toşa, F. D. Irimie, L. Poppe, C. Paizs and L. C. Bencze, ChemCatChem, 10 (2018) 2627-2633; c) E. Z. A. Nagy, S. D. Tork, P. A. Lang, A. Filip, F. D. Irimie, L. Poppe, M. I. Toşa, C. J. Schofield, J. Brem, C. Paizs and L. C. Bencze, ACS Catal. 9 (2019) 8825-8834.
[30] K. Kovács, G. Bánóczi, A. Varga, I. Szabó, A. Holczinger, G. Hornyánszky, I. Zagyva, C. Paizs, B. G. Vértessy, L. Poppe, PLoS ONE 9 (1) (2014) e85943.
[31] A. Varga, Z. Bata, P. Csuka, D. M. Bordea, B. G. Vértessy, A. Marcovici, F. D. Irimie, L. Poppe, L. C. Bencze, Studia Univ. Babes Bolyai, Ser. Chem. 63 (2017) 293−308.
[32] R. Cavicchioli, T. Charlton, H. Ertan, S. Mohd Omar, K. S. Siddiqui, T. J. Williams, Microb. Biotechnol. 4 (4) (2011) 449-460.
[33] C. Gerday, M. Aittaleb, M. Bentahir, J. P. Chessa, P. Claverie, T. Collins, Trends Biotechnol. 18 (2000) 103–107.
[34] R. Cavicchioli, K. S. Siddiqui, Enzyme Technology, Springer Science, New York, 2006, pp. 615–638.
[35] R. Cavicchioli, K. S. Siddiqui, D. Andrews, K. R. Sowers, Curr. Opin. Biotechnol. 13 (2002) 253–261.
[36] J. C. Marx, T. Collins, S. D'Amico, G. Feller, C. Gerday, Mar. Biotechnol. 9 (2007) 293–304.
[37] R. Margesin, G. Feller, Environ. Technol. 31 (2010) 835–844.
[38] J. Jeon, J. T. Kim, S. Kang, J. H. Lee, S. J. Kim, Mar. Biotechnol. 11 (2009) 307–316.
[39] S. Goto, J. Sugiyama, H. Iizuka, Mycologia, 1969, 61, 748–774.
[40] a) U.T. Bornscheuer, R.J. Kazlauskas, Hydrolases in Organic Synthesis, Regio- and Stereoselective Biotransformations, 2nd ed., Wiley-VCH, Weinheim, 2006; b) V. Gotor-Fernández, E. Busto, V. Gotor, Adv. Synth. Catal. 348 (2006) 797–812.
[41] E. Abaházi, D. Lestál, Z. Boros, L. Poppe, Molecules 21 (2016) 767.
[42] P. Csuka, Z. Boros, L. Őrfi, J. Dobos, L. Poppe, G. Hornyánszky, Tetrahedron: Asymmetry 26 (2015) 644–649.
[43] Z. Boros, P. Falus, M. Márkus, D. Weiser, M. Oláh, G. Hornyánszky, J. Nagy, L. Poppe, J. Mol. Catal. B Enzym. 85-86 (2013) 119–125.
[44] a) A. Varga, G. Bánoczi, B. Nagy, L. C. Bencze, M. I. Toşa, Á. Gellért, F. D. Irimie, J. Rétey, L. Poppe and C. Paizs, RSC: Adv. 6 (2016) 56412-56420; b) S. D. Tork, E. Z. A. Nagy, L. Cserepes, D. M. Bordea, B. Nagy, M. I. Toşa, C. Paizs, L. C. Bencze, Sci. Rep. 9 (2019) 20123.
[45] G. Bánóczi, C. Szabó, Z. Bata, G. Hornyánszky, L. Poppe, Studia Univ. Babes Bolyai, Ser. Chem. 60(4) (2015) 213–228.
[46] A. Šali, T. L. Blundell, J. Mol. Biol. 234 (1993) 779–815.
[47] G. M. Satry, M. Adzhigirey, T. Day, R. Annabhimoju, W. Sherman, J. Comput. Aid. Mol. Des. 27 (2013) 221–234.
[48] M. H. M. Olsson, C. R. Søndergard, M. Rostkowski, J. H. Jensen, J. Chem. Theor. Comput. 7 (2011) 525–537.
[49] Schrödinger Release 2018-4: Maestro, Schrödinger, LLC, New York, NY, 2018
[50] L. C. Bencze, A. Filip, G. Bánóczi, M. I. Toşa, F. D. Irimie, Á. Gellért, L. Poppe, C. Paizs, Org. Biomol. Chem. 15 (2017) 3717−3727.
[51] a) Schrödinger Release 2018-4: Glide, Schrödinger, LLC, New York, NY, 2018; b) R. A. Friesner, J. L. Banks, R. B. Murphy, T. A. Halgren, J. L. Klicic, S. T. Mainz, M. T. Repasky, E. H. Knoll, D. E. Shaw, M. Shelley, J. K. Perry, P. Francis, P. S. Shenkin, J. Med. Chem. 47 (2004), 1739-1749; c) T. A. Halgren, R. B. Murphy, R. A. Friesner, H. S. Beard, L. L. Frye, W. T. Pollard, J. L. Banks, J. Med. Chem. 47 (2004), 1750-1759.
[52] Schrödinger Release 2018-4: MacroModel, Schrödinger, LLC, New York, NY, 2018.
[53] a) Schrödinger Release 2018-4: Prime, Schrödinger, LLC, New York, NY, 2018. b) M. P Jacobson, D. L. Pincus, C.S. Rapp, T. J. F. Day, B. Honig, D. E. Shaw, R. A. Friesner, Proteins Struct. Funct. Bioinf. 55 (2004), 351-367. c) M. P. Jacobson, R. A. Friesner, Z. Xiang, B. Honig, *J. Mol. Biol.*, 320 (2002), 597-608
[54] a) Schrödinger Release 2018-4: Desmond Molecular Dynamics System, D. E. Shaw Research, New York, NY, 2018. Maestro-Desmond Interoperability Tools, Schrödinger, New York, NY, 2018 b) K. J. Bowers, E. Chow, H. Xu, R. O. Dror, M. P. Eastwood, B. A. Gregersen, J. L. Klepeis, I. Kolossvary, M. A. Moraes, F. D. Sacerdoti,

J. K. Salmon, Y. Shan, D. E. Shaw, *Proceedings of the ACM/IEEE Conference on Super-computing (SC06)*, Tampa, FL, 2006.
[55] The PyMOL Molecular Graphics System, Open source version 1.8.2.0; Schrödinger LLC
[56] T. Morita, H. Koike, Y. Koyama, H. Hagiwara, E. Ito, T. Fukuoka, T. Imura, M. Machida, D. Kitamoto, Genome Announc. 1(2) (2013) e00064-13.
[57] The UniProt Consortium, Nucleic Acids Res. 47 (2019) D506–D515.
[58] GenBank, Nucleic Acids Res. 47 (2019) D94–D99.
[59] S. H. Kim, J. W. Kronstad, B. E. Ellis, Phytochemistry, 43(2) (1996) 351−357.
[60] P. V. Subba Rao, K. Moore, G. H. N. Towers, Can. J. Biochem. 45 (1967) 1863−1872.
[61] N. A. Dima, A. Filip, L. C. Bencze, M. Oláh, P. Sátorhelyi, B. G. Vértessy, L. Poppe, C. Paizs, Studia Univ. Babes Bolyai, Ser. Chem. 61(2) (2016) 21−34.
[62] M. C. Moffitt, G. V. Louie, M. E. Bowman, J. Pence, J. P. Noel, B. S. Moore, Biochemistry 46 (2007) 1004–1012.
[63] F. C. Cochrane, L. B. Davin, N. G. Lewis, Phytochemistry 65 (2004) 1557–1564.